

Zeonex microstructured polymer optical fiber: fabrication friendly fibers for high temperature and humidity insensitive Bragg grating sensing

GETINET WOYESSA,^{1,*} ANDREA FASANO,² CHRISTOS MARKOS,¹ ALESSIO STEFANI,^{1,3} HENRIK K. RASMUSSEN,² AND OLE BANG¹

¹DTU Fotonik, Department of Photonics Engineering, Technical University of Denmark, DK-2800 Kgs. Lyngby, Denmark

²DTU Mekanik, Department of Mechanical Engineering, Technical University of Denmark, DK-2800 Kgs. Lyngby, Denmark

³Institute of Photonics and Optical Science (IPOS), School of Physics, The University of Sydney, NSW 2006, Australia

*gewoy@fotonik.dtu.dk

Abstract: In the quest of finding the ideal polymer optical fiber (POF) for Bragg grating sensing, we have fabricated and characterized an endlessly single mode microstructured POF (mPOF). This fiber is made from cyclo-olefin homopolymer Zeonex grade 480R which has a very high glass transition temperature of 138 °C and is humidity insensitive. It represents a significant improvement with respect to the also humidity insensitive Topas core fibers, in that Zeonex fibers are easier to manufacture, has better transmittance, higher sensitivity to temperature and better mechanical stability at high temperature. Furthermore, Zeonex has very good compatibility with PMMA in terms of dilatation coefficients for co-drawing applications. The Zeonex mPOF has a core and cladding diameter of 8.8 μm and 150 μm, respectively, with a hole to pitch ratio of 0.4 and a minimum propagation loss of 2.34 ± 0.39 dB/m at 690.78 nm. We have also inscribed and characterized fiber Bragg gratings (FBGs) in Zeonex mPOFs in the low loss 850 nm spectral band.

©2016 Optical Society of America

OCIS codes: (130.5460) Polymer waveguides, (060.2280) Fiber design and fabrication, (060.2270) Fiber characterization, (060.3735) Fiber Bragg gratings, (060.2370) Fiber optics sensors.

References and links

1. D. J. Webb and K. Kalli, "Polymer Fiber Bragg Gratings," in *Fiber Bragg Grating Sensors: Thirty Years From Research to Market*, A. Cusano, A. Cutolo, and J. Albert, eds. (Bentham Science, 2010).
2. D. J. Webb, "Fiber Bragg grating sensors in polymer optical fibers," *Meas. Sci. Technol.* **26**(9), 092004 (2015).
3. H. Dobb, D. J. Webb, K. Kalli, A. Argyros, M. C. J. Large, and M. A. van Eijkelenborg, "Continuous wave ultraviolet light-induced fiber Bragg gratings in few- and single-mode microstructured polymer optical fibers," *Opt. Lett.* **30**(24), 3296–3298 (2005).
4. A. Stefani, S. Andresen, W. Yuan, N. Herholdt-Rasmussen, and O. Bang, "High sensitivity polymer optical fiber Bragg grating based accelerometer," *IEEE Photonics Technol. Lett.* **24**(9), 763–765 (2012).
5. J. Jensen, P. Hoiby, G. Emilianov, O. Bang, L. Pedersen, and A. Bjarklev, "Selective detection of antibodies in microstructured polymer optical fibers," *Opt. Express* **13**(15), 5883–5889 (2005).
6. G. Emilianov, J. B. Jensen, O. Bang, P. E. Hoiby, L. H. Pedersen, E. M. Kjaer, and L. Lindvold, "Localized biosensing with Topas microstructured polymer optical fiber," *Opt. Lett.* **32**(5), 460–462 (2007).
7. C. Markos, W. Yuan, K. Vlachos, G. E. Town, and O. Bang, "Label-free biosensing with high sensitivity in dual-core microstructured polymer optical fibers," *Opt. Express* **19**(8), 7790–7798 (2011).
8. H. U. Hassan, K. Nielsen, S. Aasmul, and O. Bang, "Polymer optical fiber compound parabolic concentrator tip for enhanced coupling efficiency for fluorescence based glucose sensors," *Biomed. Opt. Express* **6**(12), 5008–5020 (2015).
9. C. Broadway, D. Gallego, G. Woyessa, A. Pospori, G. Carpintero, O. Bang, K. Sugden, and H. Lamela, "Fabry-Perot microstructured polymer optical fiber sensors for opto-acoustic endoscopy," *Proc. SPIE* **9531**, 953116 (2015).
10. S. Egusa, Z. Wang, N. Chocat, Z. M. Ruff, A. M. Stolyarov, D. Shemuly, F. Sorin, P. T. Rakich, J. D. Joannopoulos, and Y. Fink, "Multimaterial piezoelectric fibres," *Nat. Mater.* **9**(8), 643–648 (2010).

11. A. F. Abouraddy, M. Bayindir, G. Benoit, S. D. Hart, K. Kuriki, N. Orf, O. Shapira, F. Sorin, B. Temelkuran, and Y. Fink, "Towards multimaterial multifunctional fibres that see, hear, sense and communicate," *Nat. Mater.* **6**(5), 336–347 (2007).
12. H. G. Harbach, "Fiber Bragg gratings in polymer optical fibers," PhD Thesis, Lausanne, EPFL (2008).
13. C. Zhang, W. Zhang, D. J. Webb, and G. D. Peng, "Optical fiber temperature and humidity sensor," *Electron. Lett.* **46**(9), 643–644 (2010).
14. C. Zhang, X. Chen, D. J. Webb, and G. D. Peng, "Water detection in jet fuel using a polymer optical fiber Bragg grating," *Proc. SPIE* **7503**, 750380 (2009).
15. G. Woyessa, K. Nielsen, A. Stefani, C. Markos, and O. Bang, "Temperature insensitive hysteresis free highly sensitive polymer optical fiber Bragg grating humidity sensor," *Opt. Express* **24**(2), 1206–1213 (2016).
16. W. Yuan, L. Khan, D. J. Webb, K. Kalli, H. K. Rasmussen, A. Stefani, and O. Bang, "Humidity insensitive TOPAS polymer fiber Bragg grating sensor," *Opt. Express* **19**(20), 19731–19739 (2011).
17. I. P. Johnson, W. Yuan, A. Stefani, K. Nielsen, H. K. Rasmussen, L. Khan, D. J. Webb, K. Kalli, and O. Bang, "Optical fiber Bragg grating recorded in Topas cyclic olefin copolymer," *Electron. Lett.* **47**(4), 271–272 (2011).
18. C. Markos, A. Stefani, K. Nielsen, H. K. Rasmussen, W. Yuan, and O. Bang, "High-Tg TOPAS microstructured polymer optical fiber for fiber Bragg grating strain sensing at 110 degrees," *Opt. Express* **21**(4), 4758–4765 (2013).
19. G. Woyessa, A. Fasano, A. Stefani, C. Markos, K. Nielsen, H. K. Rasmussen, and O. Bang, "Single mode step-index polymer optical fiber for humidity insensitive high temperature fiber Bragg grating sensors," *Opt. Express* **24**(2), 1253–1260 (2016).
20. G. Khanarian and H. Celanese, "Optical properties of cyclic olefin copolymers," *Opt. Eng.* **40**(6), 1024–1029 (2001).
21. A. Fasano, G. Woyessa, P. Stajanca, C. Markos, A. Stefani, K. Nielsen, H. K. Rasmussen, K. Krebber, and O. Bang, "Fabrication and characterization of polycarbonate microstructured polymer optical fibers for high-temperature resistant fiber Bragg grating strain sensors," *Opt. Mater. Express* **6**(2), 649–659 (2016).
22. S. Roy, C. Y. Yue, Z. Y. Wang, and L. Anand, "Thermal bonding of microfluidic devices: Factors that affect interfacial strength of similar and dissimilar cyclic olefin copolymers," *Sens. Actuators B Chem.* **161**(1), 1067–1073 (2012).
23. J. Anthony, R. Leonhardt, A. Argyros, and M. C. J. Large, "Characterization of a microstructured Zeonex terahertz fiber," *J. Opt. Soc. Am. B* **28**(5), 1013–1018 (2011).
24. S. G. Leon-Saval, R. Lwin, and A. Argyros, "Multicore composite single-mode polymer fiber," *Opt. Express* **20**(1), 141–148 (2012).
25. A. Tuniz, R. Lwin, A. Argyros, S. C. Fleming, E. M. Pogson, E. Constable, R. A. Lewis, and B. T. Kuhlmeiy, "Stacked-and-drawn metamaterials with magnetic resonances in the terahertz range," *Opt. Express* **19**(17), 16480–16490 (2011).
26. N. Singh, A. Tuniz, R. Lwin, S. Atakaramians, A. Argyros, S. C. Fleming, and B. T. Kuhlmeiy, "Fiber draw double split ring resonators in the terahertz range," *Opt. Mater. Express* **2**(9), 1254–1259 (2012).
27. <http://www.zeonex.com/optics.aspx>.
28. Topas Advanced Polymers Inc, "Data Sheet - Topas 5013S-04," (Topas Advanced Polymers Inc., 2015), http://www.topas.com/sites/default/files/TDS_5013S_04_e_1.pdf.
29. É. Torres, M. N. Berberan-Santos, and M. J. Brites, "Synthesis, photophysical and electrochemical properties of perylene dyes," *Dyes Pigments* **112**, 298–304 (2015).
30. T. Bremner, A. Rudin, and D. G. Cook, "Melt Flow Index Values and Molecular Weight Distributions of Commercial Thermoplastics," *J. Appl. Polym. Sci.* **41**(78), 1617–1627 (1990).
31. A. Argyros, "Microstructured polymer optical fibers," *J. Lightwave Technol.* **27**(11), 1571–1579 (2009).
32. B. T. Kuhlmeiy, R. C. McPhedran, and C. Martijn de Sterke, "Modal cutoff in microstructured optical fibers," *Opt. Lett.* **27**(19), 1684–1686 (2002).
33. T. A. Birks, J. C. Knight, and P. St. J. Russell, "Endlessly single-mode photonic crystal fiber," *Opt. Lett.* **22**(13), 961–963 (1997).
34. A. Stefani, K. Nielsen, H. K. Rasmussen, and O. Bang, "Cleaving of Topas and PMMA microstructured polymer optical fibers: Core-shift and statistical quality optimization," *Opt. Commun.* **285**(7), 1825–1833 (2012).
35. A. Abang and D. J. Webb, "Demountable connection for polymer optical fiber grating sensors," *Opt. Eng.* **51**(8), 080503 (2012).
36. I.-L. Bundalo, K. Nielsen, C. Markos, and O. Bang, "Bragg grating writing in PMMA microstructured polymer optical fibers in less than 7 minutes," *Opt. Express* **22**(5), 5270–5276 (2014).
37. I.-L. Bundalo, K. Nielsen, and O. Bang, "Angle dependent Fiber Bragg grating inscription in microstructured polymer optical fibers," *Opt. Express* **23**(3), 3699–3707 (2015).
38. R. Oliveira, L. Bilro, and R. Nogueira, "Bragg gratings in a few mode microstructured polymer optical fiber in less than 30 seconds," *Opt. Express* **23**(8), 10181–10187 (2015).
39. K. E. Carroll, C. Zhang, D. J. Webb, K. Kalli, A. Argyros, and M. C. J. Large, "Thermal response of Bragg gratings in PMMA microstructured optical fibers," *Opt. Express* **15**(14), 8844–8850 (2007).
40. A. Stefani, W. Yuan, C. Markos, and O. Bang, "Narrow bandwidth 850 nm fiber Bragg gratings in few-mode polymer optical fibers," *IEEE Photonics Technol. Lett.* **23**(10), 660–662 (2011).
41. I. P. Johnson, K. Kalli, and D. J. Webb, "827nm Bragg grating sensor in multimode microstructured polymer optical fiber," *Electron. Lett.* **46**(17), 1217–1218 (2010).

1. Introduction

Polymer optical fibers (POFs) share many of the merits that conventional silica optical fibers have for sensing applications such as immunity to electromagnetic interference, small size and multiplexing capabilities. POFs have unique features over those of silica fibers for many sensing applications. These include high flexibility in bending, non-brittle nature, low Young's modulus, high elastic strain limits and high fracture toughness, giving them great potential for fiber Bragg gratings (FBGs) based high strain and acceleration sensing applications [1–4]. POFs have also excellent compatibility with organic materials, making them ideal candidates for biomedical applications [5–9]. In addition, POFs have very low processing temperature and are easy to handle, hence low processing cost and safe disposability. Moreover, the integration of metals, insulators and semiconductors structures into extended length of polymer fibers have been demonstrated [10,11].

Some polymers, such as PMMA, strongly absorb water. As a result, PMMA based POFBGs are used for developing humidity sensors as the absorption or desorption of moisture leads to a change in refractive index and size of the fiber, both of which contribute to a change in Bragg wavelength [12–15]. However, PMMA based POFBGs suffer from strong cross sensitivity to humidity when they are used to develop strain and temperature sensors. To avoid such cross sensitivity to humidity, POFBGs made from a different class of polymers called cyclo-olefin copolymers, such as Topas grade 8007 [16,17], and 5013 [18,19], have been used as they have very low affinity to water. In addition to this, cyclo-olefin copolymers have good chemical inertness to bases and acids, and many polar solvents as compared to the conventional PMMA based POFs. They have also low birefringence and superior moldability [20]. Some grades of this class of polymers have high operating temperature, such as Topas grade 5013 [18,19]. Nevertheless, it is polycarbonate mPOFs, among currently existing POFs, that have the highest operating temperature, having a glass transition temperature of 145 °C though it has affinity to water [21].

Here we demonstrate for the first time the fabrication of low loss, endlessly single mode and humidity insensitive microstructured polymer optical fiber made of Zeonex grade 480R with glass transition temperature (T_g) of 138 °C and also the first FBG inscribed in a Zeonex mPOF in the important low attenuation 850 nm region. The polymer Zeonex belongs to the class of cyclo-olefin polymers, in particular it is an amorphous homopolymer of norbornene. Although they are chemically different, Zeonex 480R shares most of Topas 5013 properties mentioned above. The difference in chemical structure lies in the presence of ethylene in Topas 5013, which is an amorphous ethylene-norbornene copolymer with a higher percentage of norbornene [22]. This makes the fabrication of Zeonex mPOF with micron sized holes and the writing of an FBG into it non-trivial, even knowing that a holey THz fiber and a step index POF could be fabricated in Zeonex [23, 24]. Our demonstration of low loss mPOF and FBG fabrication further underlines the excellent potential of Zeonex POF and mPOFs for sensing applications.

2. Advantages of Zeonex 480R over Topas 5013

Commercial Zeonex 480R rods have been used in the past not only for the fabrication of terahertz fibers [23], but also for multicore composite POFs, which consisted of Zeonex and PMMA, as Zeonex has a very good compatibility with PMMA in terms of dilatation coefficients for co-drawing applications and processing temperature [24]. Zeonex has also been used in the fabrication of drawn metamaterial fibers for the terahertz region [25, 26]. Recently, custom cast Zeonex 480R has been used as an optical cladding in the fabrication of single mode step index humidity insensitive high temperature Topas 5013 core POF [19]. At that point in time, Zeonex was worth using only as a cladding material due to its high material loss, despite combining Zeonex with different grades of various materials would have allowed obtaining the correct refractive index difference to use it as core material. In this work, the casting method has been optimized and the material loss has been significantly reduced as we

will show later in the article. This polymer is also suitable for engineering applications requiring mechanical stability at high temperature, because of its high T_g [27].

When considering fabrication of step index or all solid POFs, the differences between Topas and Zeonex are not so evident. Contrary, when micron sized air holes are included in the material to create a regular microstructure, the superior drawability of Zeonex over Topas 5013 results in a clear advantage. It allows for more degrees of freedom in fiber design as the desired microstructures can be transferred to the final fiber more efficiently. For example, the cladding holes are symmetric with only minor distorted shape compared to Topas 5013 mPOFs. Due to the better stability of the drawing process, fluctuations in the fiber diameter are also reduced. The physical properties of Zeonex 480R are indeed well suited for high quality fiber drawing. Even if the T_g of Zeonex 480R is rather close to that of Topas 5013, 134 °C [28], a preform made of Zeonex ends up to be much easier to draw. This fact is a direct consequence of Zeonex greater molecular weight, which represents an average polymer chain length. The weight-average molecular weight (M_w) of Topas 5013 was measured to be 76400 g/mol [22] whereas the M_w of Zeonex 480R is approximately 480000 g/mol [29], which is six times larger than that of Topas 5013. The melt flow index that is the flowability, of a thermoplastic material in general decreases with increasing M_w [30]. Hence, Zeonex 480R preforms tend to flow slower than Topas 5013 under similar fiber drawing conditions, thereby ensuring highly controllable and stable fiber draw processes. The other important advantage of having a higher M_w or a lower melt flow rate is that, it can allow getting a wide range of drawing temperature and stress. Thus this wide range of drawing stress enables easier tuning of the final mechanical properties of the fiber. Nevertheless, it should be noted that either too high or too low values of M_w can make the fiber drawing very challenging or even unfeasible. The M_w of Zeonex 480R is sufficiently low to avoid this potential problem. Similar information can further be found by direct examination of the melt indices for the two polymers in the respective datasheets. At 260 °C the melt volume rate of Topas 5013 is 48 cm³/10 min if a test load of 2.16 kg is used [28]. For Zeonex 480R the melt flow index is instead as low as 21 g/10 min with the same load at an even higher temperature, 280 °C [27], where the viscosity decreases when the temperature increases. Notice that, although the latter index is expressed in g/10 min, its value should not be numerically far from the corresponding melt volume rate datum, as the specific volume of Zeonex is in the range of 1.0-1.1 cm³/g, between room temperature and its processing temperatures.

3. Zeonex preform casting and characterization

3.1 Preform casting

We cast commercial Zeonex 480R plastic pellets (Zeon Corporation) into an in-house made aluminum mold to produce an optical quality solid rod. The casting conditions were optimized in order to enhance the transparency of the Zeonex preform and minimize its tendency towards yellowing for long processing time at high temperature. Although moisture absorption of Zeonex is lower than 0.01% (ASTM D570, 23°C for 24 hours) [27], preheating of the polymer granulates is required. In particular, air trapped in the pellets may form bubbles and oxygen driven discoloration in the final preform, which consequently will result in higher material losses. The best results were obtained by applying a long and stepwise preheating phase. Prior to the melting phase, we preheated the preform under vacuum for 1 day: first at a temperature well below T_g for 16 hours and then around T_g for 8 hours. This led to a low-haze preform having significantly higher clarity than the one fabricated in reference [19], where Zeonex 480R could only be used as a cladding material due its elevated transmission loss.

3.2 Refractive index measurement

The refractive index (RI) of the Zeonex 480R material used in our experiments was measured by using a commercially available ellipsometer VASE (J.A. Woollam). It covers a wavelength range of 210-1690 nm with a 5 nm and 10 nm resolutions for the range 210-1000 nm and 1000-1690 nm, respectively. The Zeonex sample used for the refractive index measurement had a disc shape with diameter of 25 mm and 10 mm thickness and with a surface roughness of 4.23 ± 0.022 nm. Cauchy model was used to fit the dispersion of the material. Figure 1(a) displays a direct comparison between the RIs of our own custom made Zeonex and the commercially available Zeonex (Zeon Corporation). The RI measurement was performed at 25 °C. As it can be seen from Fig. 1(a), our dispersion measurement is relatively close to the one obtained from the datasheet. The slight deviation between the two measured RIs could be attributed to the different molding and optimization approaches used.

3.3 Bulk material loss measurement

Bulk material propagation loss was measured within the interval 500-1600 nm based on a modified cut-back technique [21]. A 10 cm long initial cylindrical preform, which was prepared in the same way as done for the fiber drawing preform, was machined into an 8-step structure, with each step being 1 cm long as shown in the Fig. 1(b) inset. A broadband supercontinuum source (SuperK Versa, NKT Photonics) was used as an input light source. The beam divergence of the supercontinuum source is less than 5 mrad (half angle) and the beam diameter is 1 mm and 3 mm at 530 nm and 2000 nm, respectively.

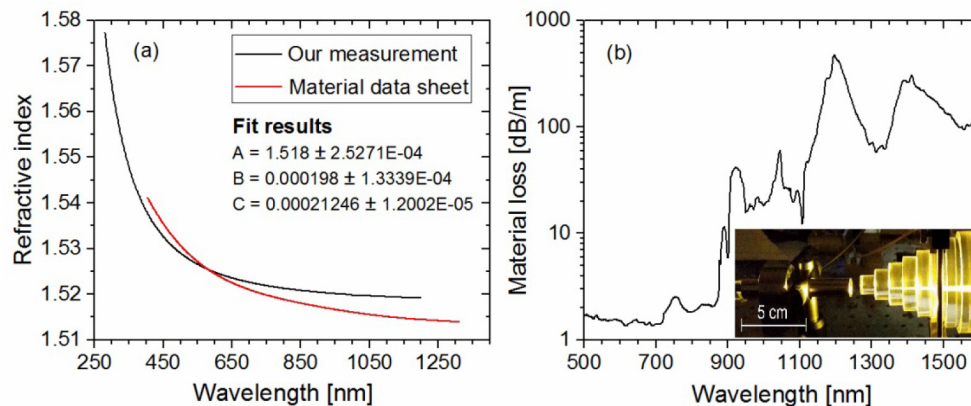


Fig. 1. (a) Material dispersion of Zeonex 480R. (b) Bulk material optical loss of Zeonex 480R. Inset: Zeonex step-like structure fabricated to measure the bulk loss.

The output light from the preform was collected and coupled to an optical spectrum analyzer (OSA, Ando AQ6315A) with a 1 mm core 2 m long multimode silica fiber patch cable (M35L02, Thorlabs) via an objective lens (10x, Zeiss). The numerical aperture of the MM fiber and the objective lens are 0.39 and 0.25, respectively. We made the measurement by recording the transmission spectrum for all step. For every step, we rotated the preform in order to record the spectrum at a different point and make sure the consistency of the measurement hence to minimize the error arising from possible surface defects on the preform or source power fluctuation. The rotation of the preform in every step was repeated five times and the final bulk loss is the average of the five measurements. Bulk material optical loss of Zeonex 480R is shown in Fig. 1(b). The material loss was relatively low in the visible range with a minimum recorded loss of 1.32 ± 0.18 dB/m at 689.98 nm while the minimum material loss for PMMA was reported to be 0.15 dB/m at 650 nm [31]. In the 500-880 nm region, the

loss was found to be less than 2.54 ± 0.21 dB/m. However, the propagation loss significantly increased in the near infrared region as shown in Fig. 1(b).

4. Endlessly single mode Zeonex mPOF fabrication and characterization

4.1 Fiber fabrication

The prepared Zeonex solid rod was first machined into a polymer preform with 100 mm length and 60 mm diameter. By using a computer numerically controlled drilling machine, 3 mm holes with a pitch of 6 mm were drilled by 60° drill in a 3-ring hexagonal arrangement. The microstructured preform was then drawn down to a 6 mm cane. The cane was sleeved by a Zeonex tube, which was also made in house, and drawn to a fiber of 150 μm average outer diameter. Both the cane and the fiber were drawn at a temperature of 180 $^\circ\text{C}$. For this temperature, the fiber drawing stress was 10 MPa. The core diameter of the fiber is 8.8 μm and the average size of holes diameter and the pitch are 2.2 μm and 5.5 μm , respectively. The hole to pitch ratio is 0.4 ensuring the fiber being endlessly single mode [32, 33]. A microscope image of the Zeonex mPOF end facet, which was cleaved with a custom made cleaver at a temperature of 78 $^\circ\text{C}$ of both blade and fiber [34], is shown as inset in Fig. 2(a).

4.2 Fiber characterization

4.2.1 Loss measurement

The transmission loss of the fabricated Zeonex mPOF was measured by cut-back method. One end of the Zeonex mPOF was connectorized [34] and connected to the visible wavelength output of a SuperK SPLIT (NKT photonics) which was connected to a supercontinuum source (SuperK Versa, NKT Photonics). The visible output of the SuperK SPLIT ranges from 450 nm to 900 nm. The light from the other end of the Zeonex mPOF was directed to a 1 mm core 2 m long multimode silica fiber patch cable via collimating (100x, Zeiss) and focusing (10x, Zeiss) objective lenses. The numerical apertures of the collimating and focusing lenses are 0.75 and 0.25, respectively, and that of the multimode fiber is 0.36. The other end of the fiber patch cable was connected to an OSA to record the Zeonex mPOF transmission spectrum. The fiber was cut back from 10 m to 50 cm, recording the transmission spectrum over 20 different fiber cuts in order to eliminate uncertainties arising from power fluctuations, coupling instabilities and cleaving quality. The measured loss profile of the Zeonex mPOF is shown in Fig. 2(a). The minimum loss was found to be 2.34 ± 0.39 dB/m at 690.78 nm. The fiber attenuation in the wavelength ranging from 550 nm to 875 nm is less than 3.2 ± 0.42 dB/m. As it can be seen in Fig. 2(a), the propagation loss of this mPOF is much lower than the previously reported microstructured [18], and step index TOPAS grade 5013 fibers [19], in particular in the visible region. The loss of our Zeonex mPOF is also much lower than the multicore step index POF having a core made of a composite of Zeonex 480R and PMMA and which has a lowest loss of 8 dB/m at 633 nm [24].

4.2.2 Fiber Bragg grating inscription and characterization

Fiber Bragg gratings were inscribed in the fabricated Zeonex mPOF in order to explore the potential of this fiber for sensing, as to our knowledge, no FBGs have been demonstrated in this material before. The grating inscription technique and the configuration setup used in this work were the same as the ones described in [36]. The phase mask used for the grating inscription in the Zeonex mPOF has a 572.4 nm uniform period, making it suitable for writing FBGs in polymers fibers in the low loss 850 nm region using a He-Cd 325 nm laser. The optimum inscription power for this fiber was found to be 5.5 mW and the corresponding writing time was less than 5 minutes. Inscription power higher than this resulted in weak gratings and also damaged the fiber, while inscription power lower than 5.5 mW resulted in longer inscription time without any improvement in the FBG strength. The writing time was shorter than the shortest writing time of 7 minutes reported for endlessly single mode PMMA

microstructured POF [36] using 30 mW CW He-Cd laser power. However, it is comparable with the inscription time of 4 minutes at a power of 6 mW (CW He-Cd laser) reported for the Topas step-index fiber [19], despite the presence of the microstructure which generally affects the writing time [37]. However, it is pertinent to note that a writing time as low as 30 seconds has been already demonstrated using a pulsed excimer laser in a few mode PMMA mPOF [38].

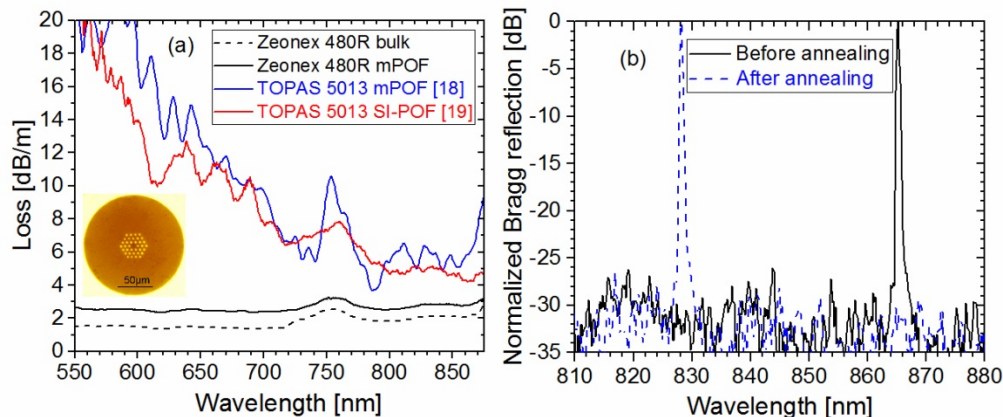


Fig. 2. (a) Measured transmission loss of bulk Zeonex 480R (dashed-black), single mode Zeonex 480R mPOF (black), single mode Topas 5013 mPOF (blue) [18], and single mode Topas 5013 SI-POF (red) [19]. Inset: microscope image of the fabricated Zeonex mPOF. (b) Bragg reflection of the Zeonex mPOF before and after annealing both normalized to the power of the non-annealed grating.

A typical reflection spectrum of a 2 mm long grating inscribed in the Zeonex mPOF is shown in Fig. 2(b). The Bragg wavelength is located at 865.24 nm with reflection strength of 30 dB and a full width half maximum of 0.522 nm. Before humidity, temperature and strain characterization, the Zeonex mPOFBG was annealed at 120 °C for 36 hours for stable operation of the sensor. After annealing, the grating blue shifted by 33.67 nm. Figure 2(b) shows the reflection spectrum of the FBG before and after annealing. Both grating reflection spectra, before and after annealing, were recorded with an optical spectrum analyzer and the spectra were then normalized to the power of the non-annealed grating. As it can be seen from Fig. 3(b) the grating was not degraded by thermal annealing.

The humidity and temperature responses of the Zeonex mPOFBG were measured using a characterization setup as described in [15]. The humidity measurement was done at 50 °C. The chamber was programmed to increase the relative humidity (RH) from 10% to 90% with a step of 10% RH. The time between each RH step was 1 hour, where 30 minutes was used to increase the RH, and 30 minutes was left for stabilization. Figure 3(a) shows the result of this process. The total wavelength change observed for the entire process was 60.2 pm and the relative humidity sensitivity measured was 0.75 ± 0.42 pm/%RH. The RH sensitivity of PMMA mPOFBG in the 850 nm region is 46 pm/%RH, which is 60 times higher than that of Zeonex mPOFBG. After reaching the value of 90% RH, the fiber was left inside the chamber for 24 hours to further investigate its humidity response. The Bragg wavelength red shifted by 8 pm in the first 4 hours of the 24 hour period and then blue shifted by 5.8 pm in the following 2 hours. These small fluctuations in the Bragg wavelength while the humidity was constant were due to the slight instability of the temperature in the chamber with time. The Bragg wavelength was almost stable in the remaining 18 hours of the constant 90% RH period as it can be seen from Fig. 3(a).

The temperature characterization was done at a fixed 50% RH by programming the chamber to increase the temperature from 20 °C to 100 °C (the maximum stable operating temperature of the chamber) and then to decrease it down to 20 °C, with steps of 10 °C

gradually within 10 minutes and stabilization time of 60 minutes. Despite the fact that we demonstrated the temperature measurement only up to 100 °C, due to the limitation of the chamber, it is possible to operate a Zeonex mPOFBG up to 115 – 120 °C as its T_g is 138 °C. Figure 3(b) shows the temperature response in the stabilization period for the range 20 °C to 100 °C at 50% RH. The temperature sensitivity of this fiber is 24.01 ± 0.1 pm/°C for both increasing and decreasing temperature. No hysteresis was observed. This is because the grating was previously annealed 20 °C higher than the maximum reached temperature. This result shows that Zeonex mPOFBG has better temperature sensitivity than that of TOPAS 5013 mPOFBG [18]. The temperature sensitivity of PMMA mPOFBG in the 1550 nm wavelength region is -52 pm/°C in the range 20 to 89 °C with a grating made in fiber pre-annealed for 7 hours at 80 °C [39].

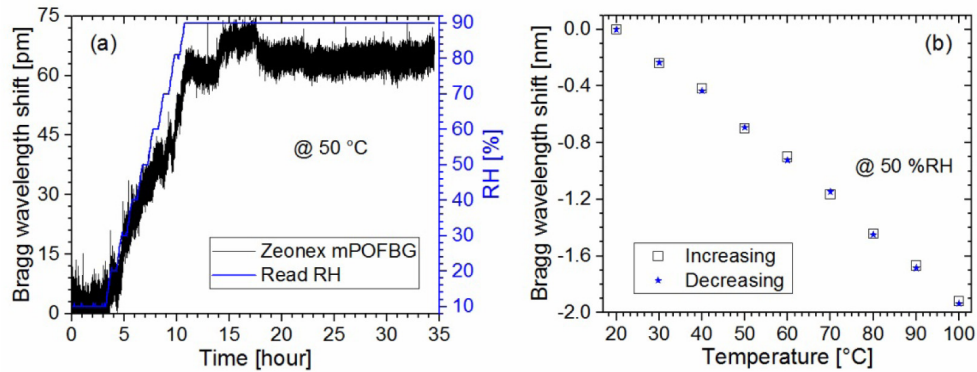


Fig. 3. (a) Humidity response at 50 °C and (b) temperature response at 50% RH of the Zeonex mPOFBG.

The strain response of the Zeonex mPOFBG was studied by mechanically elongating the grating and monitoring its reflection spectrum. A supercontinuum source (SuperK Extreme, NKT Photonics) was used as a light source and a spectrometer (CCS175-Compact Spectrometer, Thorlabs) was used to continuously track the FBG peak during strain test. The fiber was clamped and glued to two micro-translation stages, each being two centimeters away from the grating. One of the stages was used to apply axial strain to the grating manually. Every time a new strain was loaded or unloaded to the grating, 10 minutes was given to it to get stable. The fiber was longitudinally strained up to 3% with steps of 0.5%. As shown in Fig. 4, the grating shows a linear response with an R-square value of 0.999 with no hysteresis. This Zeonex mPOFBG has a strain sensitivity of 0.77 pm/ $\mu\epsilon$, for both loading and unloading cases. As expected, this value corresponds to the strain sensitivities reported for both step index and microstructured Topas 5013 POFBG [18,19] in the range 0-3% strain. In the same wavelength region, the strain sensitivities reported for a few [40] and multimode PMMA mPOFBG [41] in the range 0-2% and 0-1% strain, respectively, also match the value obtained for Zeonex mPOFBG.

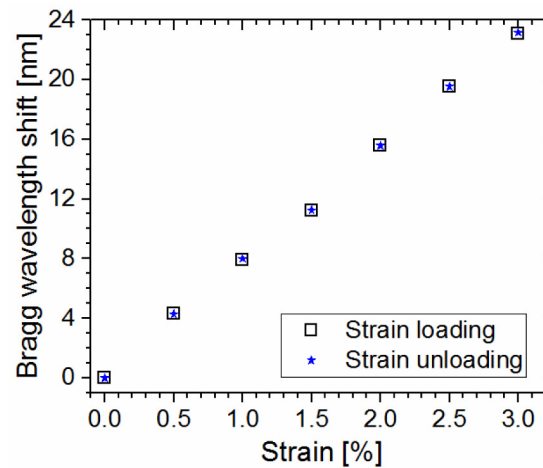


Fig. 4. Strain response of the Zeonex mPOFBG at ambient temperature and RH.

5. Conclusion

In this work, we have fabricated an endlessly single mode and humidity insensitive mPOF by the drill and drawing method. The mPOF was fabricated from norbornene homopolymer Zeonex 480R. Zeonex 480R is humidity insensitive and has a glass transition temperature of 138 °C, making it comparable with the other high operation temperature polymers for optical fibers. Two key points are related to the realization of this fiber. On one hand, the optimization of the casting method allowed reducing material loss to a level very close to other optical polymers, which eventually resulted in low fiber loss. Particularly, it provided an optical transmission one order of magnitude better in the short visible wavelengths compared to Topas core POFs. On the other hand, the higher molecular weight, compared to the ethylene-copolymerized counterpart, allowed for easier fabrication of microstructured fibers. Compared to Topas 5013, Zeonex 480R also provides a wider range of drawing temperature and stress, which gives more room for tailoring the mechanical properties of the resulting fiber to the specific application. The advantage in drawing further ensures a higher repeatability of the microstructured fiber in terms of microstructure and diameter. The realized mPOF has a core diameter and cladding diameter of 8.8 μm and 150 μm , respectively and the minimum measured material and fiber loss are 1.34 ± 0.18 dB/m and 2.34 ± 0.39 dB/m, respectively, around 690 nm. The measured average material and fiber loss in the visible wavelength range are less than 2.5 ± 0.21 dB/m and 3 ± 0.42 dB/m, respectively. A fiber Bragg grating was also inscribed in a Zeonex POF for the first time to our knowledge. The inscription process took less than 5 minutes with 5.5 mW power using a CW He-Cd laser, which we found to be the optimal power to write FBGs in this fiber. Zeonex 480R mPOFBG has shown a greater sensitivity to temperature than that of Topas 5013 mPOFBG.

The improvement in loss compared to Topas fibers allows to access working lengths over 10 m, required for most of polymer fiber sensors applications. Such achievement opens up the way to most of real life applications where the fibers cannot be embedded in water proof compounds or in applications where it is not possible to control moisture and the ambient conditions. We believe that Zeonex mPOFBGs will replace Topas-based FBGs for temperature and strain sensing with no cross sensitivity to humidity and mechanical stability at high temperature. Fiber Bragg gratings inscribed in Zeonex mPOFs are particularly suitable for engineering applications requiring mechanical stability at high temperature and very low moisture absorption. Examples of such applications would span within the automotive and composite materials. The low moisture absorption property also enables to realize high temperature and strain FBG sensor with no cross sensitivity to humidity.

Funding

People Programme (Marie Curie Actions) of the European Union's Seventh Framework Programme (608382); Danish Research Council (FTP) (4184-00359B); Eugen Lommel stipend; Marie Skłodowska-Curie grant of the European Union's Horizon 2020 research and innovation programme (708860); Carlsberg Foundation (CF14-0825) and Innovation Fund Denmark (ShapeOCT) (4107-00011A).